Experimental study of CO_2 solubility on NaCl and $CaCl_2$ solutions at 333.15 K and pressures up to 40.0 MPa

José Luiz Lara Cruz[1], François Contamine[1] and Pierre Cézac[1]

[1] Univ Pau & Pays Adour, Laboratoire de Thermique, Energetique et Procédés (LaTEP) – IPRA EA 1932, Rue Jules Ferry BP 7511, 64075 Pau Cedex, France

jose.laracruz@univ-pau.fr

Keywords: geothermal energy, CO_2 solubility, NaCl, $CaCl_2$, titration, high pressure, phase equilibria

ABSTRACT

Several projects aim to explore geothermal energy on the Upper Rhine Graben and gas solubility data are required to design the industrial installations. Thus, experimental study of CO_2 solubility on NaCl and $CaCl_2$ brines (1.2 mol NaCl/Kg H_2O and 0.2 mol $CaCl_2$/Kg H_2O) at 333.15 K has been performed. Solubility has been determined in pressure range between 6.0 MPa and 40.0 MPa with phase equilibria experiments in a well stirred reactor. Liquid samples are analysed through acid-base and conductometric titration. Literature data were used to validate our experimental protocol in order to generate original experimental points and compare them with a thermodynamic model from phreeqc software. Deviation from model can rises to 7.5% and an optimisation of the model parameters is recommended to provide more accurate data for geothermal industry.

1. INTRODUCTION

The development of renewable energies has been defined by the International Energy Agency (IEA) as one of the key strategies for reducing CO_2 emission (IEA 2016). Among all the available renewable resources, geothermal energy has received a lot of attention from scientific community being the object of industrial projects around the world.

Depending on the wells depth, geothermal energy can be either shallow (up to 2000 m of depth) or deep geothermal.

Generally on deep geothermal energy projects, heat is recovered thanks to an Enhanced Geothermal System (EGS) (Pan et al. 2018). For economic reasons, a geothermal resource must present not only high temperatures but also good ground permeability to extract the fluid (Morgan 2018), which explains why the EGS concept has been developed to increase or even create permeability at a geothermal reservoir through hydraulic fracturing, injecting fluid into the hot reservoir to recover the fluid from the well (Lu 2017).

EGS has been used to produce mainly electricity from geothermal energy in many sites around the world such as those located in the Upper Rhine Graben: Soultz (France); Landau and Insheim (Germany). Data obtained on this study were developed on the scope of several projects which aims to explore geothermal reservoirs at these three sites.

France and Germany include themselves in an international context in which geothermal energy usage for electricity production is controlled mainly by the USA, Indonesia and Philippines as one may see at figure 1, that presents the ten countries with the biggest installed capacity of geothermal energy plants for power production in 2017 (Pan et al. 2018; BP 2018). These data present electricity produced from shallow and deep geothermal, whereas specific EGS around the world are presented on figure 2 (Lu 2017).

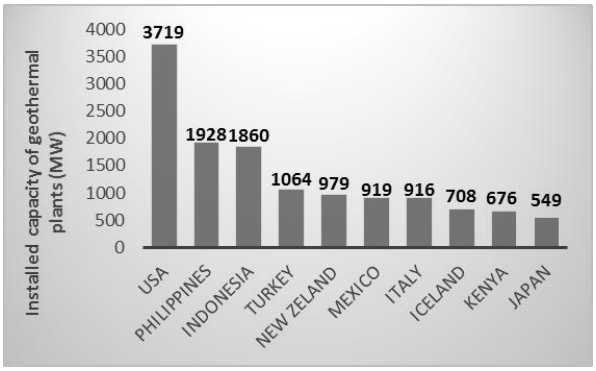

Figure 1: Ten biggest electricity world producers from geothermal energy in 2017 (Pan et al. 2018; BP 2018)

1.1. Project Context

The EGS sites located at the Upper Rhine Graben produce mainly electrical power. Well depth on these sites goes from 3000 m to 5000 m, whereas reservoir temperature can be higher than 453.15 K .All these sites work as geothermal binary plants (Lu 2017).

In a binary plant, hot fluid recovered from well is used to heat a secondary fluid in a heat exchanger. Then, the geothermal fluid is sent to the reservoir to be reheated. The secondary fluid is vaporized and used to turn a turbine or screw-expander and electrical power is produced (Morgan 2015). Then it is liquefied and resent to heat exchanger. Thus, both fluids circulate in a loop (figure 3).

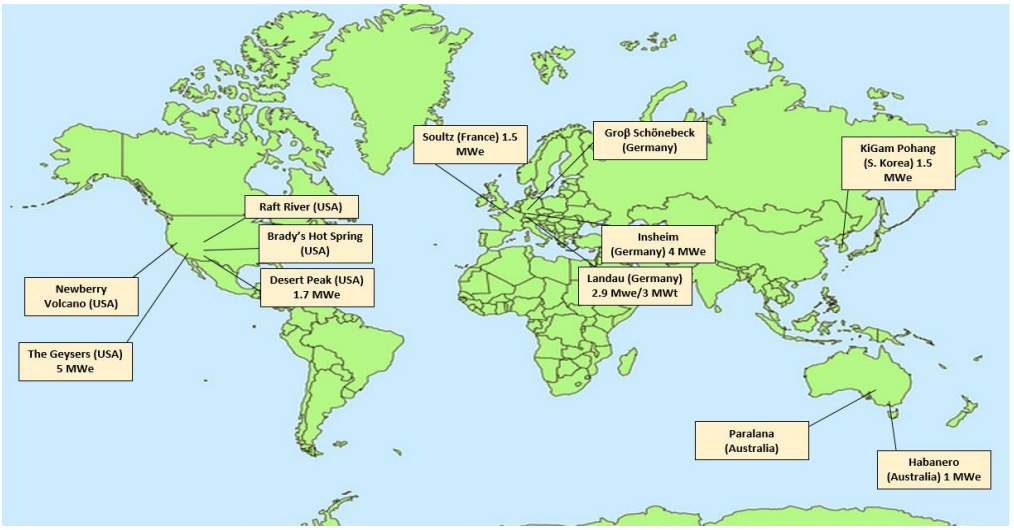

Figure 2: EGS sites around the world (Lu 2017)

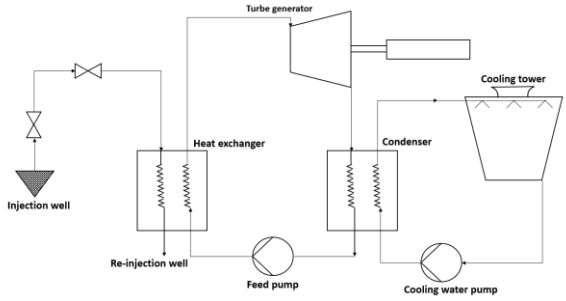

Figure 3: Diagram process for a binary geothermal plant (Global CCS Institute 2019)

Reservoirs can reach high pressures (30-40 MPa) and the gases present in the well are dissolved in the brines. When this brine is being pumped from well to the surface, its pressure decreases and a degassing process takes place. Knowledge of the pressure in which this process takes place (bubble pressure) is important to know where it is necessary to place a pump to increase fluid pressure and dissolve gases as far as possible once again. Then, most of the geothermal resource is in the liquid phase and enters the heat exchanger. Thus heat transfer and power production are more efficient.

One approach to get bubble pressure information is through gas solubility calculation thermodynamic simulation knowing the wells conditions in terms of salinity, temperature and pressure. On the other hand, thermodynamic models need high quality data to be accurate.

This study has focused on the experimental gas solubility on synthetic brines to simulate these geothermal fluids at the conditions of pressure found from fluid recovery at wells until pressures found at surface before the heat exchangers. Covered pressures go from 6.0 MPa to 40.0 MPa. Temperature chosen was 333.15 K. Even if it is not well temperature, it can be found during the pumping process of the fluid and it can provide valuable experimental data for calculating the interaction parameters in thermodynamic models.

Salt concentrations were based on those reported by Sanjuan et al. (2016) in terms of apparent chemical species for two wells located at the Graben are shown in figure 1. These compositions are representative of the Graben salinities. Synthetic brines were prepared with the most commonly found salts, that is, 1.2 mol NaCl/Kg H_2O and 0.2 mol $CaCl_2$/Kg H_2O.

Table 1: Salt concentration at two of the the Upper Rhine Graben sites (Sanjuan et al. 2016)

	Concentration in Soultz-Frace (mol/Kg H_2O)	Concentration in Isheim-Germany (mol/Kg H_2O)
NaCl	1.2240	1.3006
$CaCl_2$	0.1802	0.1820
KCl	0.0817	0.0975
$MgCl_2$	0.0053	0.0050
LiCl	0.0249	0.0242
Na_2SO_4	0.0016	0.0008

As stated by Sanjuan et al. (2016), most of the gas found is composed by CO_2 (table 2), which was chosen to be studied the molecule on the gas phase. Nevertheless, further studies concerning N_2 and CH_4 solubility are recommended. Thus, thermodynamic systems chosen for analysis were: (1) H_2O-CO_2; (2) H_2O-NaCl-CO_2; (3) H_2O-$CaCl_2$-CO_2; (4) H_2O-NaCl-$CaCl_2$-CO_2.

Table 2: Dissolved gas fraction at two of the Upper Rhine Graben sites (Sanjuan et al. 2016)

	Gas fraction at Soultz-France geothermal reservoir (%)	Gas fraction at Isheim-Germany geothermal reservoir (%)
CO_2	85.3	86.2
N_2	8.9	9.9
CH_4	2.3	2.3

Literature data are scarce for most of the temperature, pressure and salinity ranges of this project. The experimental data on literature were used to validate our experimental protocol in order to produce new data.

1.2. Literature review

Several authors have provided CO_2 solubility data in pure water data at 333.15 K and pressures from 6.0 MPa to 40.0 MPa (Bamberger et al. 2000; Bando et al. 2003; Li et al. 2004; Han et al. 2009; Guo et al. 2014; Carvalho et al. 2015; Mohammandian et al. 2015). On the other hand, CO_2 solubility has never been determined for the system H_2O-NaCl-CO_2 at the salt concentration of 1.2 mol NaCl/Kg H_2O. The closest experimental conditions to ours are for temperature of 323.15 K, pressures from 5.0 MPa to 40.0 MPa and 1 mol NaCl/Kg H_2O (Koshel et al. 2006; Yan et al. 2011; Zhao et al. 2015a; Messabeb et al. 2016).

Data for H_2O-$CaCl_2$-CO_2 and H_2O-NaCl-$CaCl_2$-CO_2 are even more difficult to be found. Gilbert et al.(2016) presents data for 0.1 mol $CaCl_2$/Kg H_2O at 335.15 K and 5.4 MPa, whereas Malinin and Saveleva (1972) exposes gas solubility for salt concentration of 0.16 mol $CaCl_2$/Kg H_2O at 353.15 K and 4.8 MPa.

Mixt brines on the Upper Rhine Graben salt concentration have not been thermodynamically characterized on the literature in terms of gas solubility. Only two works have solubility data for NaCl-$CaCl_2$ brines (Liu et al. 2011; Zhao et al. 2015b), but not on the pressure, temperature and salinity range required for this project.

Tables 3 and 4 summarizes work whose data were used for validation of our experimental apparatus, which are mainly the ones for the systems H_2O-CO_2 at 333.15 K, and H_2O-NaCl-CO_2 at 323.15 K and 1 mol NaCl/Kg H_2O. These table concern only experimental data on this project pressure range. Since the data of Li et al. (2004) are scattered from literature data at pressures higher than 10.0 MPa, it was decided that they would not be used for validation of the experimental protocol.

Data for $CaCl_2$ and NaCl-$CaCl_2$ brines were considered to be either too scarce or too far from our experimental conditions to validate our methods.

Table 3: Validation literature experimental data for the system H_2O-CO_2

Author	Temperature (K)	Pressure (MPa)
Bamberger et al.(2000)	323.15-353.15	4.1-14.1
Bando et al.(2003)	303.15-333.15	10.0-20.0
Han et al.(2009)	313.15-343.15	4.3-18.3
Guo et al.(2014)	273.15-573.15	10.0-120.0
Carvalho et al.(2015)	283.15-363.15	0.3-12.1
Mohammandian et al.(2015)	333.15-373.15	0.1-21.3

Table 4: Validation literature experimental data for the system H_2O-NaCl-CO_2

Author	Temperature (K)	Pressure (MPa)	NaCl Concentration (mol/Kg H_2O)
Koshel et al.(2006)	323.15-373.15	5.0-20.0	1-3
Yan et al.(2011)	323.15-413.15	5.0-40.0	1-5
Zhao et al.(2015a)	323.15-423.15	15.0	1-6
Messabeb et al.(2016)	323.15-423.15	5.0-200	1-6

Figures 4 and 5 present literature data exposed in tables 3 and 4 in the form of gas solubility isotherms. For both H_2O-CO_2 and H_2O-NaCl-CO_2 systems, literature data show a good agreement between them. The only point that is slightly scattered is Caravalho et al. (2015) at 10.0 MPa for pure water. However, this author points at lower pressures follow the trend of the formed isotherm by the other authors, so it was decided to use the Carvalho et al. (2015) data to validate our protocol.

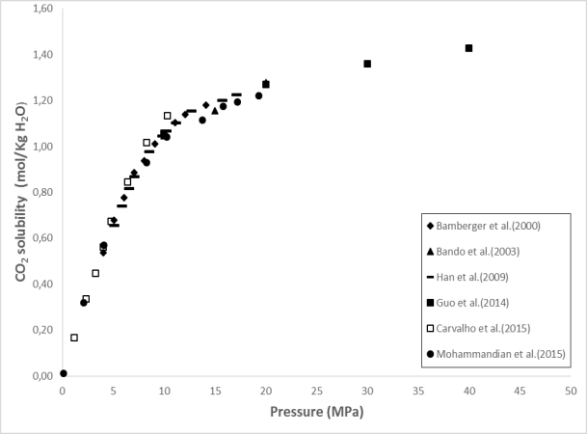

Figure 4: Literature data for solubility of CO_2 in pure water (mol CO_2/Kg H_2O) with pressure (MPa) at 333.15 K

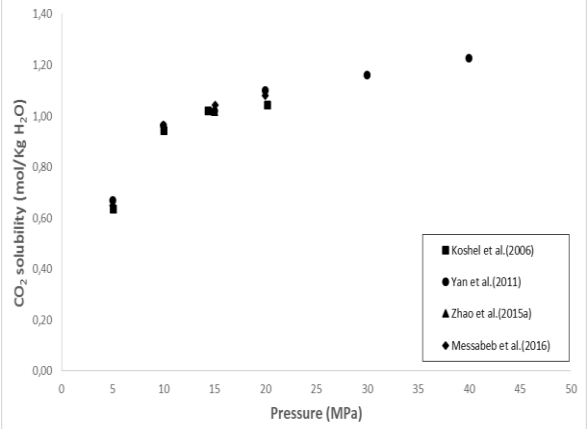

Figure 5: Literature data for solubility of CO_2 in NaCl brines (mol CO_2/Kg H_2O) with pressure (MPa) at 323.15 K and 1 mol NaCl/Kg H_2O

2. MATERIALS AND METHODS

2.1 Chemical products

Carbon dioxide (CO_2) used in this study was provided by Air Liquid in bottles containing between 5.0 and 6.0 MPa. Purity of CO_2 bottles was 99.7 %.

For the preparation of the liquid phase, water (H_2O) was purified with a water purification system from Thermo Fisher Scientific (Barnstead Smart2Pure^{TM}) until its resistivity was 18.2 MΩ.cm. Dissolved salts were sodium chloride (NaCl), and calcium chloride ($CaCl_2$), with purities of 99.5% and 96%, respectively. NaCl and $CaCl_2$ were both provided by Acros Organics.

Chemical analysis methods for CO_2 solubility required sodium hydroxide (NaOH) and hydrocloridric acid (HCl). HCl was prepared from ConvoL NORMADOSE®, acid solutions prepared by VWR Chemicals that guarantee HCl solution with concentrations ranging from 0.0995 mol/L to 0.1005 mol/L. NaOH was supplied by Fischer Scientific and used in the form of aqueous solutions, whose mass fraction can vary from 46% to 51%.

2.2 Experimental apparatus

Phase equilibria were obtained in a stirred equilibrium cell made in Hastelloy C-2000 with a volume of 250 cm^3. Maximum pressure allowed in this reactor is 55.0 MPa and temperature range goes from 273.15 K to 523.15 K. It is also conceived to support high salt concentrations such as 6 mol NaCl/ Kg H_2O and the presence of CO_2 and CH_4. The bottom of the reactor is connected to a hydraulic actuator so it can move upwards and downwards, working as a piston in order to ensure constant pressure during sampling operations.

The maximum rotation speed of the drive motor connected to two stirrers (liquid and gas phase) is 1000 revolutions per minute. The stirrers ensure homogeneity of the system as well as a lower time required to reach thermodynamic equilibrium.

The reactor is heated in three different zones. High temperatures at reactor sideways are obtained with ceramic band heaters whereas the bottom and the cover are heated with electrical resistors. Temperature is measured inside the reactor in both liquid and gas phases as well as on the cover and the bottom of the apparatus with type K thermocouples. Uncertainty of the reactor temperature measurements are estimated to be less than 1 K.

A gas compressor from Hydraulics International Inc. allows us to have the necessary high pressures for our experiments. Pressure is measured with a pressure transducer from whose pressure range is from 0 MPa to 55.0 MPa and accuracy is 0.1% of the full scale.

A vacuum pump from IMI (M/58112) is also integrated to the experimental apparatus. Reactor pressure once the pump is activated can reach 0.01 MPa.

The reactor is protected by a rupture disk and a check valve. The sampling system is composed by a high pressure two-way valve made in Hastelloy C-276, on the bottom of the cell, connected to a PEEK tube with a syringe at the end to recover the sample. Figure 6 presents a diagram of this experimental apparatus.

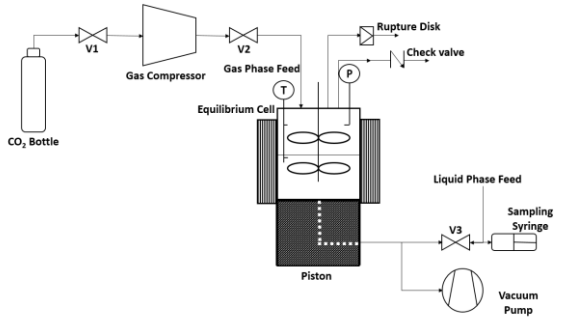

Figure 6: Process diagram of the experimental apparatus

Brines were prepared by weighing the necessary amount of ultrapure water with a Denver Instruments balance (MXX-2001) whose accuracy is 0.1 g while the salts were weighed with a Denver Instruments balance (TP-214) with accuracy of 0.0001 g, which was also used to determine the mass of the samples.

2.3 Operating Procedure

The equilibrium cell and all its lines were heated and then evacuated using the vacuum pump. This dries and eliminates any impurity that might be present before starting the equilibrium experiment. This vacuum step was also necessary to inject the liquid phase.

The reactor was set to the experiments temperature, which is 333.15 K, and then the gas compressor was turned on to increase gas pressure from 5.0 MPa to the desired pressure, which could be up to 30.0 MPa, the equipment maximum pressure. If the experiment pressure is superior to 30.0 MPa, it is necessary to load the reactor at a temperature lower than 333.15 K and then heat it in order the reach the aimed pressure.

Once liquid and gas load were performed, stirrers were activated at 800 rpm. Reactor pressure decreases since there is a mass transfer from gas to liquid phase and then it becomes completely stable when the phase equilibrium is reached, after 45 minutes.

After the 45 minutes, the PEEK tube and the syringe containing NaOH were connected to valve V3, 5 samples were collected and gas solubility was analysed through acid-base titration for the systems: (1) H_2O-CO_2; (2) H_2O-NaCl-CO_2 and conductometric titration for the remaining systems: (3) H_2O-$CaCl_2$-CO_2; (4) H_2O-NaCl-$CaCl_2$-CO_2.

2.4 Gas solubility analysis

Titrations were performed using an automatic titration unit from SI Analytics (Titroline 7800). The titrant used was HCl and CO_2 is trapped by the NaOH solution on the sampling syringe so it can react with the HCl.

The titration unit performs the chemical analysis and generates the graphic of the evolution of the pH with the added volume of titrant for the acid-base titration and the volumes required for the equivalence points are used to calculate gas solubility. When the analysis technique is the conductometric titration, the evolution of the solution conductivity is also followed with the added volume of titrant and the change in conductivity solution is used to determine the equivalence points.

For the systems free of $CaCl_2$ in which the acid-base titration is used, the chemical reactions [1] and [2] take place during the sampling process.

$$CO_2 + 2OH^- \leftrightarrow CO_3^{-2} + H_2O \qquad [1]$$

$$HCO_3^- + OH^- \leftrightarrow CO_3^{-2} + H_2O \qquad [2]$$

Sodium hydroxide is in excess in the syringe in order to convert all the CO_2 and HCO_3^- to CO_3^{-2}. The sample, containing the CO_3^{-2} and the remaining OH^-, is introduced on the titration unit and the titration graphic presented on figure 7 is obtained. During the titration three chemical reactions give us three equivalence volumes and they can be identified in order to quantify the amount of dissolved CO_2. The moments in which they take place are also indicated on the graphic.

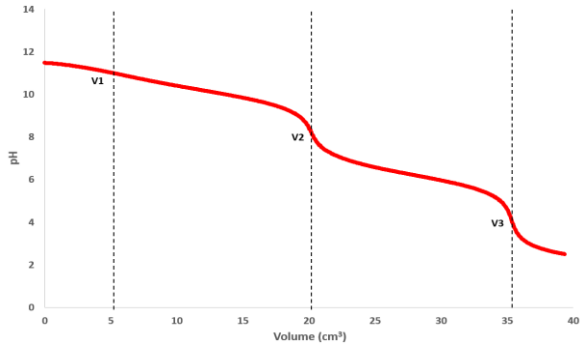

Figure 7: Typical graphical evolution of pH with titrant added volume (cm^3) for acid-base titration

The first equivalence point represents the reaction between the HCl and the excess of hydroxyl ions on the sampling syringe (reaction [3]).

$$OH^- + H^+ \leftrightarrow H_2O \qquad [3]$$

The change on the graphical slope due to this reaction is nearly imperceptible using the titration unit but it is important to state that physically this reaction takes place since the amount of sodium hydroxide introduced on the syringe was calculated to be in excess to consume all the CO_2.

Then, HCl reacts with the CO_3^{-2} to convert it to HCO_3^- (reaction [4]).When this chemical conversion is completed, there is the second equivalence point, which is graphically visible, around pH 8.5 (figure 7).

$$CO_3^{-2} + H^+ \leftrightarrow HCO_3^- \qquad [4]$$

The third and final equivalence point represents the total conversion of HCO_3^- into carbonic acid, H_2CO_3 (equation [5]) and it appears around pH 4.

$$HCO_3^- + H^+ \leftrightarrow H_2CO_3 \qquad [5]$$

Since all the CO_2 on the sample was converted to CO_3^{-2}, the difference between the two first equivalence volumes can be used to calculate the gas solubility. However, since the first slope rupture is not visually perceptible, it is the difference between the two last equivalence points (graphically visible) that is used to calculate gas solubility. This calculation is possible because the $CO_3^{-2}$is entirely converted to HCO_3^-during the second chemical reaction. If the mass of water (m_{H_2O}) withdrawn with the sample is kwon as well as the equivalence volumes (V_1-V_2-V_3) and the HCl concentration (C_{HCl}), it is possible to calculate the CO_2 solubility through equation [1].

$$C_{CO_2} = C_{CO_3^{-2}} = \frac{C_{HCl}*(V_2-V_1)}{m_{H_2O}} = C_{HCO_3^-} = \frac{C_{HCl}*(V_3-V_2)}{m_{H_2O}} \qquad [1]$$

When $CaCl_2$ is present on the brine (systems H_2O-$CaCl_2$-CO_2 and H_2O-NaCl-$CaCl_2$-CO_2), it forms a solid precipitation ($CaCO_3$) with the CO_2. This precipitation interferes with the pH probe and decreases the quality of its signal and thus the accuracy of the measure. Therefore, for those systems it is essential to have the additional conductivity probe on the analysis unit.

Due to the presence of the Ca^{2+} ions, the chemical reactions during the sampling process are slightly different with the formation of $CaCO_3$. In addition to the reactions [1] and [2], there is also the conversion of CO_3^{-2} to $CaCO_3$ (reaction [6]).

$$CO_3^{-2} + Ca^{2+} \leftrightarrow CaCO_{3(sd)} \qquad [6]$$

Thus, the syringe contains $CaCO_3$ and the excess of NaOH that did not react with the CO_2. This sample is introduced in the titration unit and two equivalence points divide the graphic in three regions (figure 8). The pH evolution was followed as supplementary information.

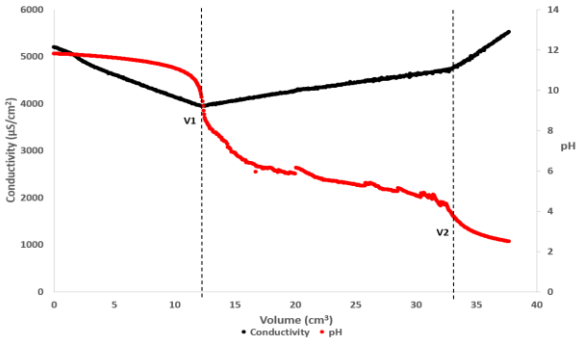

Figure 8: Typical graphical evolution of pH and conductivity (µS/cm^2) with the titrant added volume (cm^3) for a conductometric titration

The first zone corresponds to the reaction between the hydroxyl ions in excess with the HCl (reaction [3]), as it happens for the acid-base titration but in this case the slope change is visually perceptible. This zone is recognized by the constant decrease on the solution conductivity.

The phenomenon on the second region is the $CaCO_3$ dissolution (reaction [7]), that ends at the second equivalence volume. This zone is characterized by an increase on the solution conductivity.

$$CaCO_{3(sd)} + 2H^+ \leftrightarrow Ca^{2+} + H_2CO_3 \quad [7]$$

The knowledge of this two equivalence points is necessary for the CO_2 solubility calculation. The final zone on the graphic represents the addition of H^+ ions once the $CaCO_3$ is consumed. At this moment, no chemical reaction takes place anymore and conductivity increases with a different slope due to the excess of H^+ present on the titration unit.

Since all the CO_2 was initially converted into $CaCO_3$, the two equivalence volumes (V_2-V_1) represent the dissolution of the $CaCO_3$ and can be used to calculate the CO_2 (equation [2]) if the quantity of ultrapure water (m_{H_2O}) withdrawn with the sample and the HCl concentration (C_{HCl}) are known.

$$C_{CO_2} = C_{CaCO_3} = \frac{C_{HCl} * (V_2 - V_1)}{2 * m_{H_2O}} \quad [2]$$

For both titrations, sampling was repeated 5 times and the average was considered to be the CO_2 solubility.

2.5 Solubility measurements uncertainties

Solubility measurements uncertainties were determined using ANOVA method, which will not be described here but the reader is invited to check the literature to have further details (Feinberg and Laurentie 2010; Messabeb 2017).

ANOVA method allow us to evaluate how much of the experiment uncertainty is due to the repeatability and the reproducibility of it. In other words, if the experiment uncertainty is mainly due to the repetition of the chemical analysis (repeatability) or due to the reproduction of the pressure and temperature conditions for each experiment (reproducibility).

Therefore, it was decided that a same experiment would be reproduced 3 times and the chemical analysis would be repeated 8 times in order to have 24 titrations. The uncertainty calculated with these 24 titrations is considered to be uncertainty of all our experiments. The system chosen to estimate the experimental uncertainty was H_2O-CO_2 at 333.15 K and 10.0 MPa.

The uncertainty obtained with ANOVA method is 2.8%. Errors due to reproducibility of the experiments are considered to be negligible. The Student factor for a confidence level of 95% and two degrees of freedom was used as coverage factor on this uncertainty calculation.

3. RESULTS AND DISCUSSION

The first solubility data produced were useful for validation of the operating procedure. CO_2 solubility was thus analysed in conditions that could be easily found on literature in order to optimize and validate the experimental handling protocol.

As stated previously on the section *1.2 Literature Review*, chosen systems for the validation step were: (1) H_2O-CO_2 at 333.15 K; (2) H_2O-NaCl -CO_2 at 1 mol NaCl/Kg H_2O and 323.15 K. Both systems were studied at pressures up to 40.0 MPa. Once our data agreed with literature, it was possible to extrapolate the operating protocol for the other systems of interest of this project. Tables 5 and 6 present solubility data obtained as well as the average deviation from literature data reported previously on this paper for each set of experimental conditions. Figures 9 and 10 present these data in the form of gas solubility isotherms.

Table 5: Experimental data for CO_2 solubility in pure water at 333.15 K

Pressure (MPa)	Gas solubility (mol CO_2/Kg H_2O)	Gas solubility uncertainty (mol CO_2/Kg H_2O)	Literature Deviation (%)
6.07	0.75	0.02	2.29
10.07	1.04	0.03	2.02
20.00	1.27	0.04	0.54
25.06	1.32	0.04	*
30.05	1.36	0.04	0.27
40.08	1.50	0.04	4.84

*No available literature data

Table 6: Experimental data for CO_2 solubility in 1 mol NaCl/Kg H_2O brines at 323.15 K

Pressure (MPa)	Gas solubility (mol CO_2/Kg H_2O)	Gas solubility uncertainty (mol CO_2/Kg H_2O)	Literature Deviation (%)
5.07	0.62	0.02	5.40
10.05	0.91	0.03	5.13
20.02	1.06	0.03	3.31
29.99	1.13	0.03	2.39
40.04	1.28	0.04	3.72

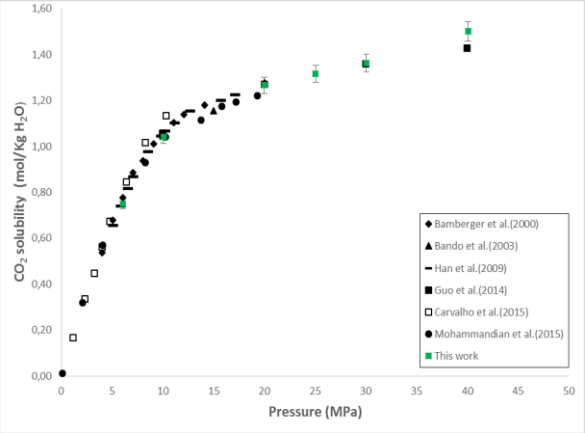

Figure 9: CO_2 solubility (mol/Kg H_2O) in pure water compared to literature data at 333.15 K

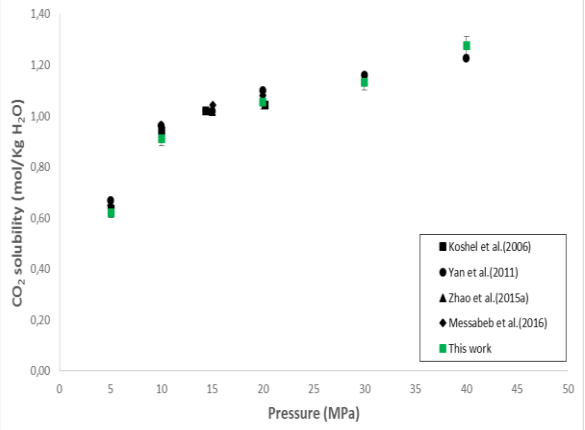

Figure 10: CO_2 solubility (mol/Kg H_2O) in 1 mol NaCl/Kg H_2O brine compared to literature data at 323.15 K

In both cases, CO_2 solubility increases with pressure. Its increase is stronger and almost linear for pressures up to 10.0 MPa and the graphical slope decreases gradually for higher pressures. Literature deviation with our experimental data was considered to be adequate for both thermodynamic systems and the operating procedure was validated.

Considering pure water results, the biggest average deviation was 4.84 % at 40.0 MPa, when this study data is compared to the result of Guo et al. (2014). Since there is only this author in literature presenting a 40.0 MPa point, a deviation lower than 5% was considered acceptable. Otherwise, results at 6.0 MPa, 10.0 MPa, 20.0 MPa and 30.0 MPa are even better and presented less than 2.29 % of deviation with literature data.

For the system containing NaCl, average literature deviation is lower than 5.4% for any pressure studied and even inferior to 3.7% for pressures above 20.0 MPa. Average deviation around 5% observed for 6.0 MPa and 10.0 MPa is mainly due to the deviation with the points of Yan et al. (2011) at 6.0 MPa, which is 8.09% and Messabeb et al. (2016) at 10.0 MPa, which is 6.04%. At these pressures, deviations with Koshel et al. (2006) are 3.25 % at 6.0 MPa and 3.65% at 10.0 MPa. Thus, the average of all deviation from these authors is about 5% for both pressures and the operating protocol is considered acceptable for systems containing dissolved salts.

Then, CO_2 solubility data was produced for the other thermodynamic systems of interest on the context of this project. Experimental results were compared to calculation performed by phreeqc software using the PITZER.DAT database (table 7 and figures 11, 12, 13).

Table 7: Experimental data for CO_2 solubility in NaCl, $CaCl_2$ and mixt brines at 333.15 K

	Pressure (MPa)	Gas solubility (mol CO_2/Kg H_2O)	Uncertainty (mol CO_2/Kg H_2O)	Phreeqc deviation (%)
H_2O-NaCl - CO_2 1.2 mol NaCl/Kg H_2O	6.01	0.62	0.02	1.07
	10.01	0.87	0.02	4.34
	20.01	1.00	0.03	1.19
	29.97	1.04	0.03	6.19
	39.97	1.13	0.03	3.70
H_2O-$CaCl_2$-CO_2 0.2 mol $CaCl_2$/Kg H_2O	6.09	0.74	0.02	5.78
	10.05	1.01	0.03	5.69
	20.08	1.26	0.04	7.56
	30.06	1.33	0.04	4.49
	40.02	1.45	0.04	6.63
H_2O-NaCl-$CaCl_2$-CO_2 1.2 mol NaCl-0.2 mol $CaCl_2$/Kg H_2O	6.06	0.58	0.02	1.28
	10.01	0.81	0.02	4.69
	20.07	0.97	0.03	3.00
	30.02	1.06	0.03	3.18
	40.05	1.14	0.03	3.97

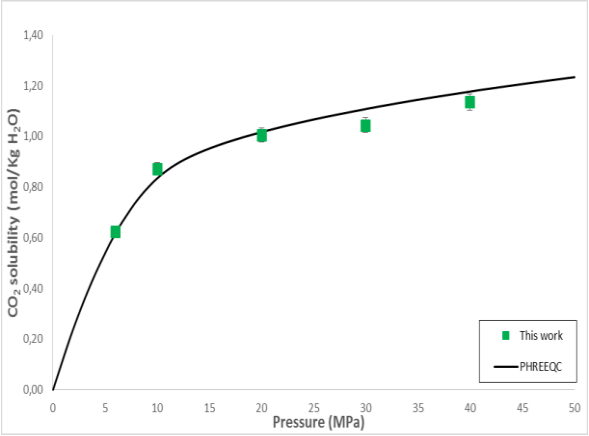

Figure 11: CO_2 solubility (mol/Kg H_2O) in 1.2 mol NaCl/Kg H_2O brine at 333.15 K compared to phreeqc calculation

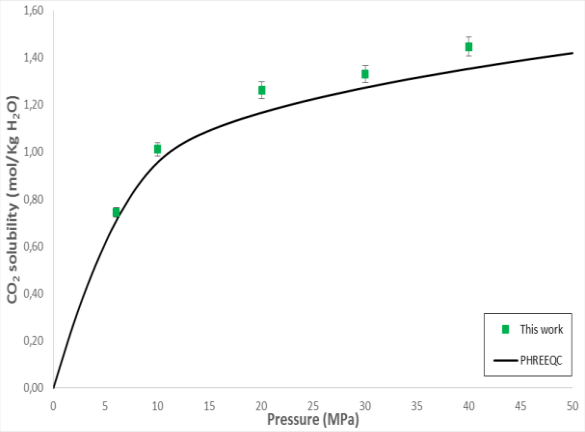

Figure 12: CO_2 solubility (mol/Kg H_2O) in 0.2 mol $CaCl_2$/Kg H_2O brine at 333.15 K compared to phreeqc calculation

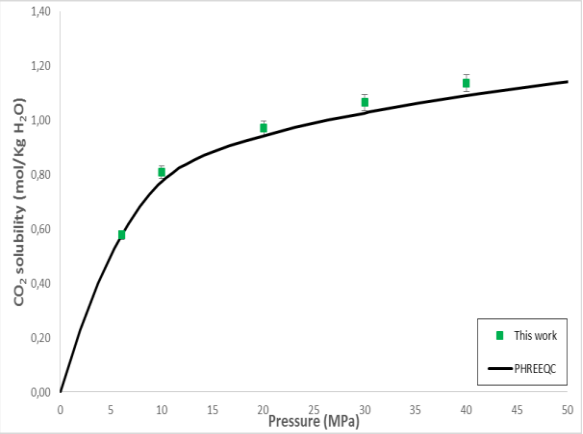

Figure 13: CO_2 solubility (mol/Kg H_2O) in 1.2 mol NaCl-0.2 mol $CaCl_2$/Kg H_2O brine at 333.15 K compared to phreeqc calculation

From all the 15 data exposed on table 7, only 3 points agree with phreeqc within 2.8%, our study uncertainties. This means that an optimisation of the model thermodynamic interaction parameters would be recommended for the three systems using the experimental data presented here. However, it is important to remark that deviation from phreeqc is smaller for the 1.2 mol NaCl/Kg H_2O brine and for the salt mixture NaCl/$CaCl_2$ brine on the pressure range of this project.

Indeed, for the NaCl brine, deviation goes from 1.07% to 4.34% except for the point at 29.97 MPa, in which there is a deviation of 6.19%.However, considering the measurements uncertainties, this points follows the trend of the experimental isotherm, which follows the model within a maximum deviation of 4.3%.

For the salt mixture brine, deviation goes from 1.28% to 4.69% without any exception, which shows a better agreement between experimental data and model than for the NaCl brine. Phreeqc model indicates a difference of 6% between CO_2 solubility on the salt mixture brine and on the NaCl brine. Experimental data for the mixt brine are, in average, 3.22% above model calculation. Since experimental data for the NaCl brine are generally below model calculation, the solubility difference between the two brines would be smaller than what is announced by phreeqc.

On the other hand, deviations for the system H_2O-$CaCl_2$-CO_2 are higher, ranging from 4.49% to 7.56%, which means the software would under estimate the CO_2 solubility in this brine. An overall analysis of the three systems could indicate that most of the deviation observed for the salt mixture brine when compared to phreeqc comes from the $CaCl_2$ thermodynamic parameters since CO_2 solubility calculation for the $CaCl_2$ brine is less accurate than for the NaCl brine.

Studying the effect of each salt separately is interesting to point out which one of them is the most implicated on the salting out effect of the liquid phase at the studied salinities. The salting out effect is the phenomenon in which gas solubility decreases in a liquid phase due to the increase of its salt concentration (Koshel et al. 2006; Yan et al. 2011; Zhao et al.2015; Messabeb et al.2016; Kim et al.2016).

Literature reports different ways of quantifying the salting out effect, such as the Setschenow constant (Mohammandian et al. 2015; Kim et al. 2016) or the relative deviation between gas solubility in pure water and on the brine (Koshel et al.2006; Mohammandian et al. 2015; Messabeb et al.2017). The second methodology was chosen (equation [3]). In this equation, S_0 is the CO_2 solubility in pure water, and S is the solubility in the studied brine.

$$S.O._{\%} = \frac{100*(S_0 - S)}{S_0} \qquad [3]$$

Figure 14 shows the CO_2 solubility difference between pure water and the NaCl/$CaCl_2$ salt mixture brine in which one can clearly see that a salting out effect exists. Furthermore, this CO_2 solubility decrease represents about 24% of initial solubility and it is mainly due to the NaCl present on the brine since $CaCl_2$ salting out effect of our experiments ranges from 1% to 4% (figure 15). Thus, the addition of $CaCl_2$ results in a decrease in CO_2 solubility within its uncertainty measurements.

The consequence of it is that by performing an experiment in which $CaCl_2$ is added to the liquid phase, one may not see any significant effect even though CO_2 solubility decreases. This is illustrated in figure 15 by comparing salting out effect in NaCl brine and salt mixture brine at 30.0 MPa and 40 MPa, in which NaCl brine salting out is higher than on the NaCl/$CaCl_2$ brine, whereas one would expect the opposite. Physically one cannot deny that the addition of 0.2 mol of $CaCl_2$ decreases gas solubility on liquid phase. However, since the $CaCl_2$ salting out effect lies within the experimental solubility uncertainties, it is expected that, at some point in a series of experiments this kind of observation occurs.

Another demonstration of this phenomenon are the $CaCl_2$ salting out effect uncertainties that would indicate a negative salting out effect (figure 15) while

what happens is that the $CaCl_2$ salting out effect exists but it is not strong and rarely exceeds 4%.Uncertainties expressed in figure 15 were obtained with the uncertainty propagation principle on the equation 3.

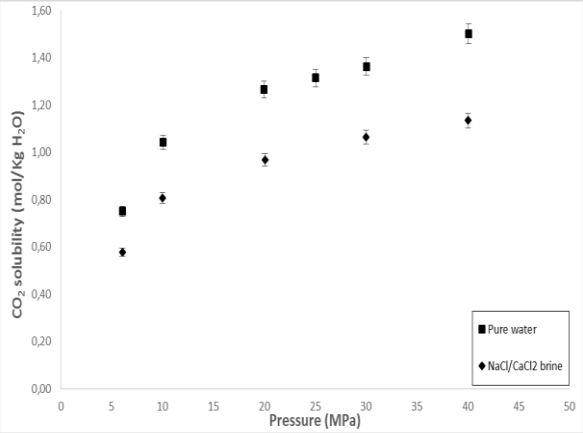

Figure 14: Comparison between CO_2 solubility (mol/Kg H_2O) in pure water and salt mixture brine at 333.15 K

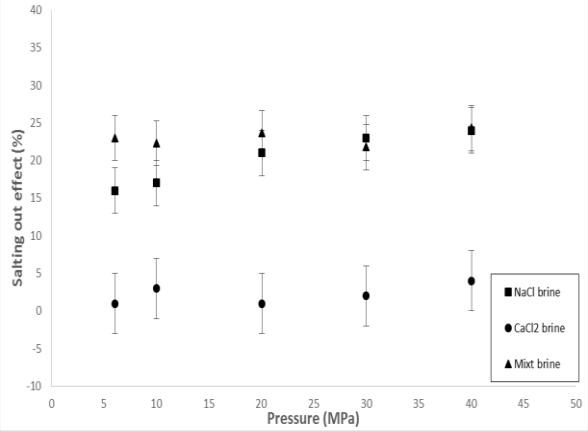

Figure 15: Comparison of the salting out effect (%) for the different salinities of this study in terms of pressure (MPa)

Results seem to indicate that the difference between the CO_2 solubility in the NaCl and the salt mixture brine is smaller than the one announced by phreeqc. However, this difference exists and it is recommended to perform experiments with the salts mixture rather than just the NaCl.

4. CONCLUSIONS

CO_2 solubility data in pure water and NaCl/$CaCl_2$ brines are required for geothermal industry projects on the Upper Rhine Graben. However, literature review has revealed a lack of experimental data for brines with the specific salinities found on the Graben. Since the CO_2 solubility depends on the brine salinity, an experimental device was developed to determine CO_2 solubility in pure water, NaCl, $CaCl_2$ and salt mixture brines with phase equilibria experiments.

An experimental handling protocol was developed to determine CO_2 solubility in brines for 333.15 K and pressures from 6.0 MPa to 40.0 MPa. Salinities used were 1.2 mol NaCl/Kg H_2O and 0.2 mol $CaCl_2$ mol/Kg H_2O. Measurements uncertainties were estimated to be 2.8% with ANOVA method.

Main results concern the solubility points produced for the systems H_2O-NaCl-CO_2, H_2O-$CaCl_2$-CO_2 and H_2O-NaCl-$CaCl_2$-CO_2 at the Graben salinities. Comparison with phreeqc indicates that an optimisation of the thermodynamic parameters for the software model could be done at the temperature, pressure and salinity range of this project. Model deviation is higher for the $CaCl_2$ brine.

Salting out effect produced by the salt mixture rises to 24% and most comes from NaCl. Indeed, NaCl brines present an average salting out effect of 20% whereas $CaCl_2$ brines salting out effect ranges from 1% to 4%.

Finally, it would be interesting for the continuation of this work to perform experiments at higher temperature (at least 423.15 K) since well temperatures at the Upper Rhine Graben are higher than 453.15 K.

REFERENCES

Bamberger, A., Sieder, G. and Maurer, G.: High-pressure (vapour+liquid) equilibrium in binary mixtures of (carbon dioxide+water or acetic acid) at temperatures from 313 to 353 K, *The Journal of Supercritical Fluids*, **17**, (2000), 97-110

Bando, S., Takemure, F., Nishio M., Hihara E. and Akai, M.: Solubility of CO_2 in aqueous solutions of NaCl at (30 to 60) °C and (10 to 20) MPa, *Journal of Chemical Engineering Data*, **48**, (2003), 576-579

BP: 2018 Statistical Review of World Energy, available online at: https://www.bp.com/en/global/corporate/energy-economics/statistical-review-of-world-energy.html (accessed February 05, 2019)

Carvalho, P.J., Pereira, L.M.C, Gonçalves, N.P.F., Queimada, A.J and Coutinho, J.A.P.: Carbon dioxide solubility in aqueous solutions of NaCl: Mesurements and modeling with electrolyte equations of state, *Fluid Phase Equilibria*, **388**, (2015), 100-106

Feinberg, M. and Laurentie, M.: Validation methods for quantitative analysis through the accuracy profile, *INRA technical handbook 2010 version*, Institut National de la Recherche Agronomique-INRA, Jouy-en- Josas,(2010), 144p. Avaiable online at : https://intranet.inra.fr/cahier_des_techniques (accessed February 20,2019)

Gilbert, K., Bennett P.C, Wolfe, W., Zhang, T. and Romanak, K.: CO_2 solubility in aqueous solutions containing Na^+, Ca^{2+} , Cl^-, SO_4^{-2} and HCO_3^-. The effects of electrostriced water and ion hydratation thermodynamics, *Applied Geochemistry*, **67**, (2016), 59-67

Global CCS Institute: Binary cycle power plants, available online at:

https://hub.globalccsinstitute.com/publications/geothermal-electricity-and-combined-heat-power/binary-cycle-power-plants (accessed February 07, 2019)

Guo, H., Chen, Y., Hu, Q., Lu, W., Ou, W. and Geng, L.: Quantitative Raman spectroscopic investigation of geo-fluids high-pressure phase equilibria: part I. Accurate calibration and determination of CO_2 solubility data in water from 273.15 to 573.15K and from 10 to 120 MPa, *Fluid Phase Equilibria*, **382**, (2014), 70-70

Han, J.M., Shin, H. Y., Min, B.M., Han, K.H. and Cho, A.: Measurement and correlation of high pressure phase behavior of carbon dioxide+water system, *Journal of Industrial and Engineering Chemistry*, **15**, (2009), 212-216

IEA, International Energy Agency,: Energy Technology Perspectives 2016: Towards Sustainable Urban Energy Systems, *International Energy Agency*, Paris , (2016)

Kim, K., Seo, K., Lee, J., Kim, M.G. and Ha, K.S.: Investigation and prediction of the salting-out effect of methane in various aqueous electrolyte solution, *Journal of Industrial and Engineering Chemistry*, **34** , (2016), 117-121

Koshel, D., Coxam, J.Y., Rodier, L. and Majer, V.: Enthalpy and solubility data of CO_2 in water and NaCl (aq) at conditions of interest for geological sequestration, *Fluid Phase Equilibria*, **247**, (2006), 107-120

Li, Z., Dong, M., Li, S. and Dai, L.: Densities and Solubilities for Binary Systems of Carbon Dioxide+Water and Carbon Dioxide+Brine at 59°C and Pressures at 29 MPa, *Journal of Chemical Engineering Data*, **49**, (2004), 1026-1031

Liu, Y., Hou, M., Yang, G. and Han, B.: Solubility of CO_2 in aqueous solutions of NaCl, KCl and $CaCl_2$ and their mixed salts at different temperatures and pressures, *Journal of Supercritical Fluids*, **56**, (2011), 125-129

Lu, S.M.: A global review of enhanced geothermal system (EGS), *Renewable and Sustainable Reviews*, **81**, (2017), 2902-2921.

Malinin, S.D. and Saveleva, N.I.: Investigation of CO_2 solubility in NaCl and $CaCl_2$ solutions at temperatures of 25,50 and 75 degrees and elevated CO_2 pressure, *Geokhimiya*, **6**, (1972), 643-653

Messabeb, H., Contamine, F., Cézac, P., Serin, J.P. and Gaucher, E.C.: Experimental measurement of CO_2 solubility in aqueous NaCl solution at temperature from 323.15 to 423.15 K and pressure of up to 20 MPa, *Journal of Chemical Engineering Data* , **61**, (2016), 3573-3584

Messabeb, H., Contamine, F., Cézac, P., Serin, J.P., Pouget, C. and Gaucher, E.C. : Experimentl measurement of CO_2 solubility in aqueous $CaCl_2$ solutions at temperatures from 323.15 to 423.15 K and pressures up to 20 MPa using the conductometric titration, *Journal of Chemical Engineering Data*, **62**, (2017), 4228-4234

Messabeb, H.: Thermodynamical characterization of liquid-vapor equilibria for CO_2-brines systems at high temperatures-high pressures conditions, *PhD Thesis on Engineering Process*, Univ Pau & Pays Adour, Pau ,(2017), 142p.

Mohammandian, E., Hamidi H., Asadullah, M., Azdarpout A., Motamedi, S. and Junin, R.: Measurements of CO_2 solubility in NaCl Brine Solutions at Different Temperatures and Pressures Using Potentiometric Titration Method, *Journal of Chemical Engineering Data*, **60**, (2015), 2042-2049

Morgan, P.: Geothermal Energy, in: American Association of Petroleum Geologists, Energy Minerals Division: Unconventional Energy Ressources: 2015 Review, *Natural Resources Research*, **24**, (2015), 458-466

Morgan, P.: Geothermal Energy, in :American Association of Petroleum Geologists, Energy Minerals Division: Unconventional Energy Ressources : 2017 Review, *Natural Resources Research*, (2018), 50-58

Pan, S.Y., Gao, M., Shah, K.J.., Zheng, J., Pei, S.L. and Chiang, P.C.: Establishement of enhanced geothermal energy utilization plans: barriers and strategies, *Renewable Energy*, (2018)

Sanjuan, B., Milot, R., Innocent, Ch., Dezayes, Ch., Scheiber, J. and Brach, M.: Major geochemical characteristics of geothermal brines from the Upper Rhine Graben granitic basement with constraints on temperature and circulation, *Chemical Geology*, **428**, (2016), 27-47

Yan, W., Huang, S. and Stenby, E.H.: Measurement and modelling of CO_2 solubility in NaCl brine and CO_2-saturated NaCl brine density, *International Journal of Greenhouse Gas Control*, **5**, (2011), 1460-1477

Zhao, H., Fedkin, M.V., Dilmore, R.M. and Lvov, S.N.: Carbon dioxide solubility in aqueous solutions of sodium chloride at geological conditions: Experimental results at 323.15, 373.15, and 423.15 K and 150 bar and modeling up to 573.15 K and 2000 bar, *Geochimica and Cosmochimica Acta*, **149**, (2015a), 165-189

Zhao, H., Dilmore, R., Allen D.E., Hedges, S.W., Soong Y. and Lvov, S.N.: Measurement and Modeling of CO_2 Solubility in Natural and Synthetic Formation Brines for CO_2 sequestration, *Environmental Science & Technology*, **49**, (2015b), 1972-1980

Acknowledgements

The authors would like to thank ADEME and the Carnot ISIFoR Institute for the funding of this project.